Supporting Information

Is the Isolated Pentagon Rule Always Satisfied for Metallic Carbide Endohedral Fullerenes?

Tao Yang,[†] Xiang Zhao,[†,*] Sheng-Tao Li,[†] and Shigeru Nagase[‡]

Content

I. Relative energies of Tetra-anions C_{84}^{4-} of both IPR and non-IPR isomers.

II. Relative energies and HOMO-LUMO gaps of $Y_2C_2@C_{84}$ isomers.

III. Cartesian coordinates of $Y_2C_2@D_{2d}(51591)$-C_{84} and $Y_2C_2@C_1(51383)$-C_{84}.

IV. Theoretical ^{13}C NMR chemical shifts of $Y_2C_2@C_1(51383)$-C_{84} and $Y_2C_2@D_{2d}(51591)$-C_{84}.

V. Theoretical simulated UV-vis-NIR spectra of $Y_2C_2@C_1(51383)$-C_{84} and $Y_2C_2@D_{2d}(51591)$-C_{84}.

VI. Full reference of Ref. 27.

I. Relative energies of Tetra-anions C_{84}^{4-} of both IPR and non-IPR isomers.

In order to assign the cage structure of $Y_2C_2@C_{84}$, we have performed extensive semi-empirical calculations on the tetra-anions of both IPR isomers and non-IPR isomers with number of fused pentagons less than three at AM1 level. The total number of these isomers is 1193. Here we only provide the isomers with the relative energy less than 40 kcal/mol. For all the calculated results, please contact the corresponding author.

Table S1. Relative energies of tetra-anions C_{84}^{4-}.

Spiral ID	Symmetry	PA[a]	Charge State	ΔHf kcal/mol	$\Delta\Delta Hf$ kcal/mol
51591	D_{2d}	0	-4	1160.14	0.00
51589	D_2	0	-4	1160.34	0.19
51578	C_s	0	-4	1165.20	5.05
51580	C_1	0	-4	1165.52	5.37
51590	D_2	0	-4	1166.15	6.00
51575	C_{2v}	0	-4	1168.70	8.55
51581	C_2	0	-4	1170.57	10.42
51583	C_s	0	-4	1172.88	12.73
51573	D_2	0	-4	1177.10	16.96
51577	C_2	0	-4	1177.13	16.98
51579	C_2	0	-4	1178.64	18.49
51576	C_2	0	-4	1179.70	19.56
51571	C_s	0	-4	1182.56	22.42
51587	D_{3d}	0	-4	1183.38	23.23
51584	C_s	0	-4	1185.92	25.78
51574	C_{2v}	0	-4	1192.25	32.10
51585	C_{2v}	0	-4	1194.73	34.59
51592	D_{6h}	0	-4	1195.11	34.97
51572	D_{2d}	0	-4	1197.78	37.63
51582	C_s	0	-4	1199.56	39.42
51383	C_1	1	-4	1175.79	15.64
51483	C_1	1	-4	1178.87	18.73
51499	C_1	1	-4	1179.66	19.52
51482	C_1	1	-4	1180.64	20.50
51365	C_s	1	-4	1181.00	20.85
51550	C_s	1	-4	1181.24	21.10
51539	C_1	1	-4	1184.11	23.97
45206	C_1	1	-4	1184.33	24.19
51353	C_1	1	-4	1184.41	24.26
51425	C_s	1	-4	1185.97	25.83
51481	C_1	1	-4	1186.14	26.00

51397	C_1	1	-4	1186.41	26.27
43990	C_1	1	-4	1186.62	26.47
51422	C_1	1	-4	1187.21	27.07
51350	C_1	1	-4	1187.62	27.48
51519	C_s	1	-4	1187.89	27.75
49167	C_1	1	-4	1188.31	28.17
49805	C_1	1	-4	1188.33	28.18
51546	C_s	1	-4	1191.10	30.95
43979	C_1	1	-4	1191.39	31.25
51401	C_1	1	-4	1192.28	32.13
51496	C_1	1	-4	1192.36	32.22
51545	C_{2v}	1	-4	1193.95	33.81
51348	C_1	1	-4	1194.59	34.44
50769	C_1	1	-4	1194.69	34.54
50322	C_2	1	-4	1195.39	35.25
43947	C_1	1	-4	1195.53	35.39
43959	C_1	1	-4	1196.07	35.93
51538	C_1	1	-4	1196.15	36.00
45512	C_1	1	-4	1196.59	36.44
50525	C_1	1	-4	1196.62	36.48
45084	C_1	1	-4	1197.04	36.89
47391	C_1	1	-4	1197.21	37.07
50244	C_1	1	-4	1197.94	37.80
51416	C_1	1	-4	1198.38	38.23
51536	C_s	1	-4	1198.47	38.32
51543	C_1	1	-4	1199.42	39.28
51368	C_1	1	-4	1199.55	39.40
51036	C_1	1	-4	1199.58	39.44
51551	C_s	2	-4	1192.92	32.78
46283	C_1	2	-4	1195.81	35.66
51434	C_s	2	-4	1195.83	35.69
51433	C_1	2	-4	1196.95	36.81
46281	C_1	2	-4	1197.24	37.10
46282	C_1	2	-4	1198.50	38.35

a: PA: the number of pentagon adjacencies.

II. Relative energies and HOMO-LUMO gaps of $Y_2C_2@C_{84}$ isomers.

Metallic carbide EMFs $Y_2C_2@C_{84}$ were firstly optimized at B3LYP level of theory with 3-21G basis set for C atoms and Lanl2dz basis set with the CEP effective core potential (ECP) for Y). Then the molecular structures of $Y_2C_2@C_{84}$ were re-optimized at B3LYP level with a larger basis set 6-31G(d) for C.

Table S2. Relative energies and HOMO-LUMO gaps of $Y_2C_2@C_{84}$ isomers.

$Y_2C_2@C_{84}$			B3LYP 3-21G-Lanl2dz		B3LYP 6-31G(d)-Lanl2dz	
Spiral ID	Symmetry	PA	ΔE kcal/mol	Gap eV	ΔE kcal/mol	Gap eV
51589	D_2	0	8.70	1.15	8.39	1.13
51591	D_{2d}	0	0.00	1.64	0.00	1.59
51383	C_1	1	1.81	1.79	4.93	1.71
51483	C_1	1	7.13	1.86	10.63	1.78
51499	C_1	1	7.55	1.35	10.42	1.33
51365	C_s	1	5.61	1.31	12.30	0.00
46283	C_1	2	12.85	1.66	24.05	1.63

III. Cartesian coordinates of $Y_2C_2@D_{2d}$(51591)-C_{84} and $Y_2C_2@C_1$(51383)-C_{84}.

The molecular structures of $Y_2C_2@D_{2d}$(51591)-C_{84} and $Y_2C_2@C_1$(51383)-C_{84} were optimized at B3LYP/6-31G(d)-Lanl2dz level of theory.

$Y_2C_2@D_{2d}$(51591)-C_{84}:

C	-0.023571	-0.037509	0.110276
C	1.433673	-0.024834	0.108060
C	2.191526	1.169922	0.092928
C	3.450826	1.212858	-0.685795
C	3.877182	2.494222	-1.241262
C	4.387195	2.513810	-2.607842
C	3.960986	3.722439	-3.227305
C	3.782970	3.815038	-4.650736
C	2.842099	4.772920	-5.095133
C	2.100913	4.560109	-6.300667
C	0.730347	4.960783	-6.098761
C	-0.350545	4.189628	-6.606427
C	-1.595854	4.155691	-5.832609
C	-2.488474	3.001633	-5.951126
C	-3.313676	2.626527	-4.865533
C	-3.591840	1.225517	-4.573758
C	-3.621819	1.089579	-3.137719
C	-3.210858	-0.085167	-2.537124
C	-2.464253	-0.033268	-1.311573
C	-1.632792	-1.213089	-1.296062
C	-0.434992	-1.209870	-0.605497
C	0.720137	-1.874185	-1.157072

C	1.864375	-1.183231	-0.633111
C	3.036162	-1.142750	-1.365057
C	3.841021	0.051153	-1.391820
C	4.478762	0.100446	-2.706263
C	4.653434	1.331379	-3.380811
C	4.517522	1.394708	-4.839577
C	4.081136	2.641447	-5.477061
C	3.440586	2.558563	-6.745829
C	2.398036	3.480768	-7.117571
C	1.343884	2.772941	-7.778799
C	-0.010157	3.075284	-7.501821
C	-0.929631	1.979373	-7.625049
C	-2.124084	1.942256	-6.849811
C	-2.473395	0.553528	-6.628464
C	-3.117002	0.173110	-5.382430
C	-2.678563	-1.080994	-4.741788
C	-2.746356	-1.191881	-3.337735
C	-1.733552	-1.890293	-2.555905
C	-0.762395	1.164463	0.005123
C	-2.018989	1.194813	-0.751102
C	-2.454946	2.441894	-1.389283
C	-3.297563	2.349316	-2.530125
C	-3.213649	3.306578	-3.607035
C	-2.405875	4.421889	-3.485507
C	-1.649300	4.895054	-4.618595
C	-0.494351	5.554202	-4.077602
C	0.679408	5.587323	-4.806119
C	1.953000	5.443491	-4.149258
C	2.035667	5.248081	-2.751499
C	3.175730	4.479905	-2.260896
C	3.172959	3.745430	-1.004728
C	1.917951	3.689808	-0.253991
C	1.445301	2.407038	0.237894
C	-0.005571	2.376947	0.130119
C	-0.428589	3.584598	-0.488634
C	-1.632190	3.649897	-1.266311
C	-1.658846	4.636258	-2.280403
C	-0.454554	5.368777	-2.648662
C	0.777357	5.205241	-1.973253
C	0.752998	4.382738	-0.777021
C	-0.583778	-2.440543	-3.168804
C	0.703878	-2.412780	-2.473499
C	1.946060	-2.368931	-3.251996
C	3.095082	-1.791988	-2.646102

C	4.072764	-1.069964	-3.422159
C	3.982766	-1.042793	-4.805204
C	4.275906	0.170508	-5.524218
C	3.503037	0.119207	-6.735559
C	3.091190	1.295313	-7.336455
C	1.785077	1.386587	-7.934811
C	0.894125	0.282201	-7.935905
C	-0.527160	0.606971	-7.921564
C	-1.527497	-0.283781	-7.347117
C	-1.093340	-1.523829	-6.713045
C	-1.634028	-1.845306	-5.402787
C	-0.586729	-2.448846	-4.604625
C	0.615685	-2.433088	-5.368654
C	1.893908	-2.361502	-4.720297
C	2.927913	-1.749214	-5.467052
C	2.629679	-1.024490	-6.702765
C	1.337472	-0.984799	-7.288465
C	0.328989	-1.838574	-6.671956
C	0.103630	0.872344	-3.186713
C	-0.185348	1.955457	-3.769744
Y	-0.162534	0.296039	-5.475034
Y	1.609398	2.509497	-2.320400

$Y_2C_2@C_1(51383)$-C_{84}:

C	-0.009402	-0.066785	0.089013
C	1.412155	-0.078048	0.130128
C	2.147868	1.172763	0.098442
C	3.334594	0.958114	-0.656545
C	3.880448	1.981655	-1.469204
C	4.677110	1.528282	-2.570860
C	4.877543	2.324078	-3.729335
C	5.076723	1.449489	-4.864758
C	4.568687	1.855545	-6.151852
C	3.912806	0.835465	-6.946504
C	2.675515	1.189046	-7.613438
C	1.807404	0.057588	-7.584964
C	0.378895	0.191707	-7.616659
C	-0.352906	-0.858127	-7.009641
C	-1.599750	-0.591406	-6.352037
C	-1.695252	-1.373715	-5.157185
C	-2.255933	-0.819895	-3.973637
C	-1.778315	-1.364984	-2.751122

C	-1.819127	-0.610217	-1.546121
C	-0.675763	-1.012010	-0.738747
C	-0.661399	1.188810	0.313594
C	-1.912576	1.514829	-0.376387
C	-2.352326	0.709396	-1.494144
C	-2.766426	1.374609	-2.761618
C	-2.755805	0.564268	-3.980930
C	-2.754939	1.247704	-5.219896
C	-2.144633	0.675282	-6.396220
C	-1.484857	1.712466	-7.141718
C	-0.186752	1.536938	-7.691008
C	0.701858	2.710790	-7.751552
C	2.158260	2.527120	-7.689858
C	2.975885	3.539980	-7.127869
C	4.099423	3.187490	-6.267534
C	4.094187	4.104371	-5.143483
C	4.327812	3.636006	-3.820075
C	3.524305	4.139799	-2.699403
C	3.237703	3.288220	-1.539041
C	2.047316	3.531331	-0.717640
C	1.516327	2.447067	0.143242
C	0.101951	2.423625	0.495483
C	-0.756308	3.495617	0.082271
C	-1.972965	2.942878	-0.469955
C	-2.260912	3.604682	-1.712548
C	-2.666630	2.842985	-2.876142
C	-2.441531	3.487189	-4.175002
C	-2.587104	2.673644	-5.308173
C	-1.881376	2.952406	-6.538355
C	-1.082621	4.058464	-6.647412
C	0.191692	3.962053	-7.320345
C	1.036539	4.969002	-6.726917
C	2.406647	4.753158	-6.623951
C	3.100072	5.099018	-5.399946
C	2.406460	5.662545	-4.341600
C	2.633470	5.204875	-2.992113
C	1.415090	5.371207	-2.269053
C	1.125380	4.611508	-1.121079
C	-0.283860	4.515252	-0.796531
C	-1.270444	4.660105	-1.857442
C	-0.925912	5.221962	-3.118690
C	-1.603039	4.708415	-4.304108
C	-0.988242	4.986458	-5.547042
C	0.316597	5.598826	-5.638861

C	0.999220	5.963274	-4.479270
C	0.372662	5.778698	-3.211985
C	2.156892	-1.050558	-0.613311
C	3.378711	-0.435319	-1.044919
C	4.022838	-0.843660	-2.237988
C	4.755574	0.145253	-2.962710
C	4.992309	0.070004	-4.393847
C	4.339953	-0.970567	-5.190269
C	3.809082	-0.555993	-6.493391
C	2.478883	-1.010139	-6.895340
C	1.708912	-1.974973	-6.154570
C	0.295997	-1.909462	-6.255126
C	-0.535520	-2.231379	-5.122259
C	0.037708	-2.633282	-3.889739
C	-0.644026	-2.244376	-2.702685
C	0.064413	-1.987960	-1.477514
C	1.495008	-2.014443	-1.439222
C	2.181528	-2.455930	-2.617439
C	3.442773	-1.903723	-2.995721
C	3.538056	-1.903155	-4.446718
C	2.283344	-2.459220	-4.939113
C	1.462076	-2.788871	-3.823310
C	0.769579	2.247951	-4.280464
C	0.441957	1.068600	-3.971902
Y	-0.158063	2.251377	-1.983734
Y	2.606983	0.708042	-4.806246

IV. Theoretical ^{13}C NMR chemical shifts of $Y_2C_2@C_1(51383)$-C_{84} and $Y_2C_2@D_{2d}(51591)$-C_{84}.

To simulate the ^{13}C NMR chemical shifts of $Y_2C_2@C_1(51383)$-C_{84}, we employed the gauge-independent atomic orbital (GIAO) method. The ^{13}C NMR chemical shifts were evaluated at B3LYP/6-311G(d)-Lanl2dz level of theory. Theoretical chemical shift values have been calibrated to the observed C_{60} line (142.50 ppm). The two [5,5]-carbons (41 and 42) exhibit two signals at 160.2 and 161.6 ppm, respectively, in very good conformity with the experimentally values of 160.6 and 161.7 ppm. It's noteworthy that because the encapsulated carbide moiety rotates fast inside the fullerene cage, the chemical shifts of these two carbon atoms (86 and 87) are difficult to be simulated theoretically. For $Y_2C_2@D_{2d}(51591)$-C_{84}, according to its Cs symmetry, there are only 44 signals in the ^{13}C NMR spectrum, including 42 full-intensive and 2 half-intensive ones. Especially, the chemical shifts of the carbon atoms in the fullerene cage range from 130 to 154 ppm. Thus, the ^{13}C NMR spectrum of $Y_2C_2@D_{2d}(51591)$-C_{84} doesn't match the experimental spectrum.

Table S3. Computed ^{13}C NMR chemical shifts of $Y_2C_2@C_1(51383)$-C_{84}.

Atoms	Chemical Shift ppm	Intensity	Atoms	Chemical Shift ppm	Intensity
1	130.7	1	43	146.7	1
2	143.6	1	44	131.3	1
3	134.0	1	45	130.4	1
4	140.4	1	46	142.1	1
5	129.0	1	47	129.2	1
6	133.8	1	48	134.3	1
7	133.4	1	49	139.9	1
8	127.0	1	50	152.0	1
9	132.6	1	51	142.8	1
10	132.7	1	52	149.4	1
11	139.7	1	53	149.0	1
12	139.1	1	54	148.8	1
13	131.6	1	55	145.3	1
14	142.6	1	56	128.4	1
15	145.4	1	57	143.6	1
16	148.7	1	58	147.9	1
17	141.4	1	59	133.4	1
18	148.5	1	60	137.2	1
19	141.6	1	61	143.6	1
20	138.4	1	62	155.7	1
21	148.5	1	63	148.6	1
22	142.0	1	64	141.0	1
23	130.5	1	65	156.8	1
24	125.1	1	66	144.1	1
25	138.1	1	67	135.6	1
26	144.6	1	68	140.5	1
27	148.5	1	69	134.4	1
28	143.9	1	70	145.2	1
29	137.2	1	71	137.2	1
30	137.7	1	72	135.9	1
31	132.5	1	73	132.3	1
32	149.6	1	74	147.3	1
33	149.1	1	75	160.5	1
34	154.4	1	76	142.7	1
35	134.6	1	77	155.6	1
36	134.5	1	78	153.8	1
37	135.3	1	79	147.5	1
38	122.1	1	80	150.3	1
39	129.4	1	81	142.6	1
40	144.9	1	82	133.1	1
41	160.2	1	83	137.7	1

42	161.6	1		84	146.4	1	
85	287.2	1					
86	261.3	1					

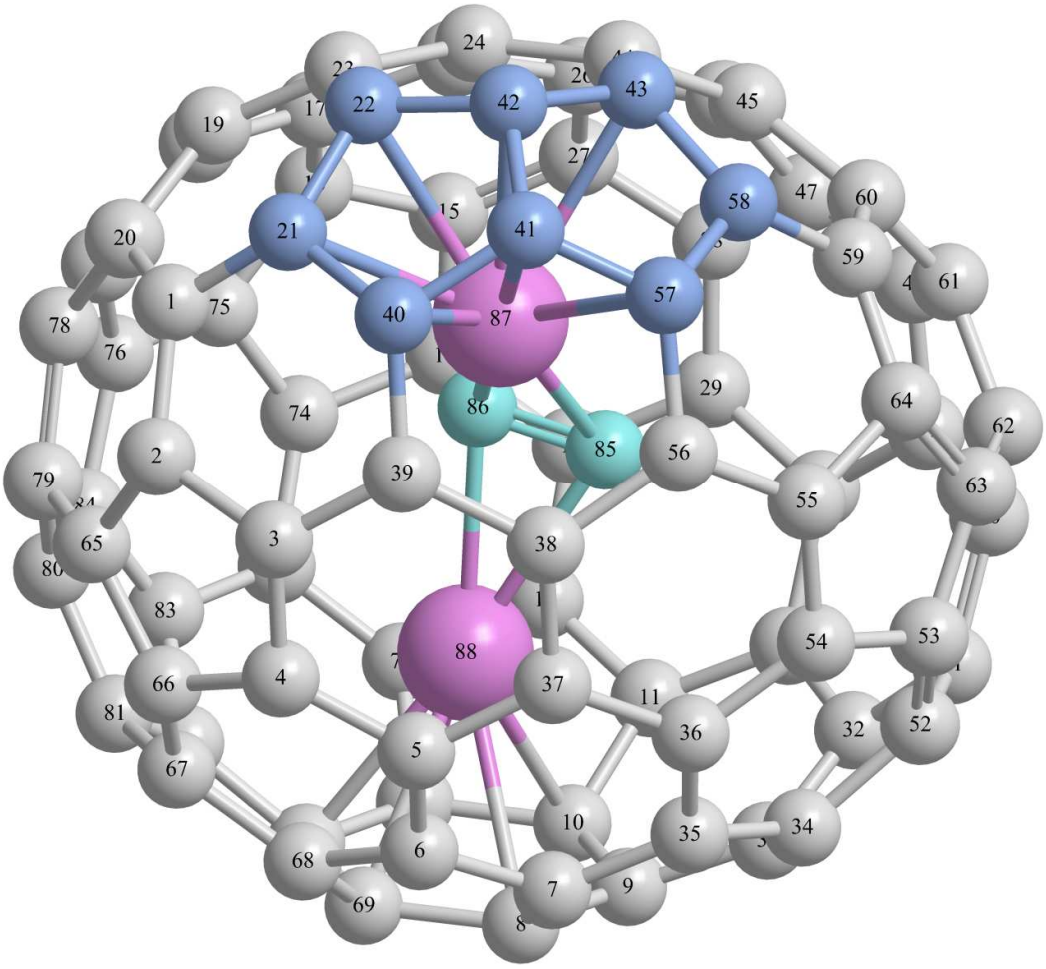


Figure S1. Optimized molecular structure of $Y_2C_2@C_1(51383)$-C_{84}.

Table S3. Computed ^{13}C NMR chemical shifts of $Y_2C_2@D_{2d}(51591)$-C_{84}.

Chemical Shifts	Intensity		Chemical Shifts	Intensity		Chemical Shifts	Intensity
ppm			ppm			ppm	
152.36	2		139.77	2		139.25	1
150.37	2		139.55	2		134.12	1
149.46	2		139.25	2			
148.55	2		138.79	2			
148.54	2		138.79	2			
148.47	2		137.82	2			
146.37	2		137.56	2			

145.08	2		137.12	2			
145.05	2		136.27	2			
144.91	2		135.87	2			
144.59	2		135.14	2			
144.27	2		134.97	2			
143.68	2		134.56	2			
143.12	2		133.61	2			
142.94	2		133.29	2			
142.93	2		133.15	2			
142.63	2		132.93	2			
141.67	2		131.40	2			
141.51	2		130.96	2			
140.38	2		130.83	2			
140.17	2	C2	279.09	2			

V. Theoretical simulated UV-vis-NIR spectra of $Y_2C_2@C_1$(51383)-C_{84} and $Y_2C_2@D_{2d}$(51591)-C_{84}.

Using time-dependent density functional theory, we simulated the UV-vis-NIR spectra of both $Y_2C_2@C_1$(51383)-C_{84} and $Y_2C_2@D_{2d}$(51591)-C_{84}, as shown in Figure S2. It's found that UV-vis-NIR spectrum of $Y_2C_2@C_1$(51383)-C_{84} is close to the experimental one. For instance, the spectrum of $Y_2C_2@C_1$(51383)-C_{84} is rather featureless with two weak absorption bands (500-600 nm and 630-750 nm), in agreement with the experimental spectrum of $Y_2C_2@C_{84}$, since there are also few absorption band in the spectrum of $Y_2C_2@C_{84}$. In contrast, for the spectrum of $Y_2C_2@D_{2d}$(51591)-C_{84} only one highly intensive absorption band presents in the region from 500 to 700 nm. Moreover, there is also an obvious absorption band in 1170 nm.

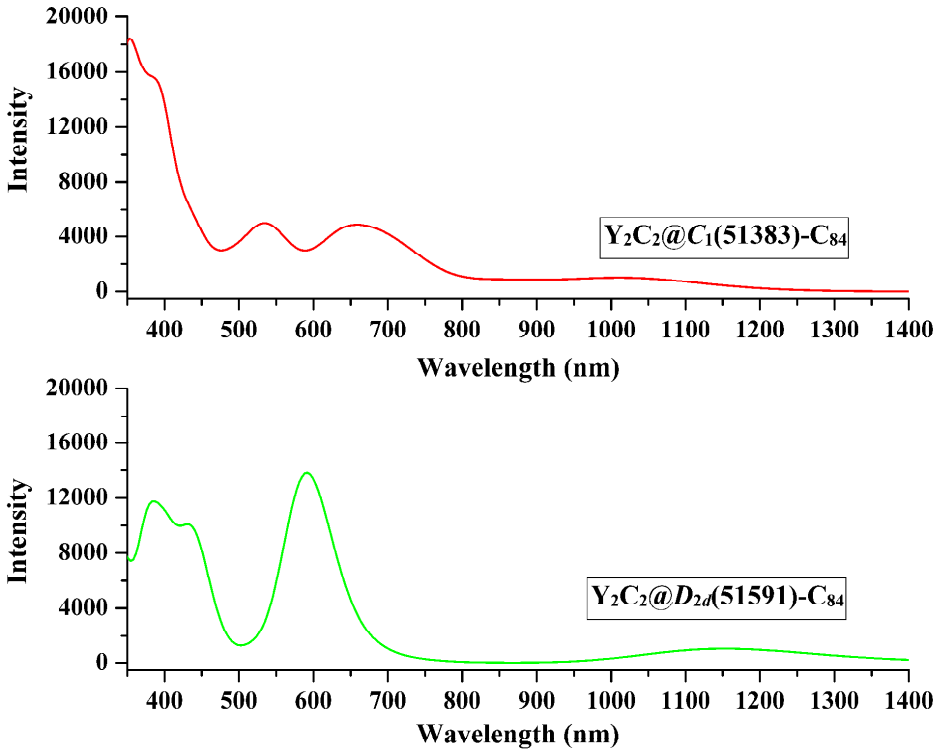


Figure S2. Simulated UV-vis-NIR spectra of $Y_2C_2@C_1(51383)$-C_{84} and $Y_2C_2@D_{2d}(51591)$-C_{84}.

VI. Full reference of Ref. 27

Frisch, M. J.; Trucks, G. W.; Schlegel, H. B.; Scuseria, G. E.; Robb, M. A.; Cheeseman, J. R.; Montgomery, J. A.; Vreven, J. T.; Kudin, K. N.; Burant, J. C.; Millam, J. M.; Iyengar, S. S.; Tomasi, J.; Barone, V.; Mennucci, B.; Cossi, M.; Scalmani, G.; Rega, N.; Petersson, G. A.; Nakatsuji, H.; Hada, M.; Ehara, M.; Toyota, K.; Fukuda, R.; Hasegawa, J.; Ishida, M.; Nakajima, T.; Honda, Y.; Kitao, O.; Nakai, H.; Klene, M.; Li, X.; Knox, J. E.; Hratchian, H. P.; Cross, J. B.; Bakken, V.; Adamo, C.; Jaramillo, J.; Gomperts, R.; Stratmann, R. E.; Yazyev, O.; Austin, A. J.; Cammi, R.; Pomelli, C.; Ochterski, J. W.; Ayala, P. Y.; Morokuma, K.; Voth, G. A.; Salvador, P.; Dannenberg, J. J.; Zakrzewski, V. G.; Dapprich, S.; Daniels, A. D.; Strain, M. C.; Farkas, O.; Malick, D. K.; Rabuck, A. D.; Raghavachari, K.; Foresman, J. B.; Ortiz, J. V.; Cui, Q.; Baboul, A. G.; Clifford, S.; Cioslowski, J.; Stefanov, B. B.; Liu, G.; Liashenko, A.; Piskorz, P.; Komaromi, I.; Martin, R. L.; Fox, D. J.; Keith, T.; Al-Laham, M. A., Peng, C. Y.; Nanayakkara, A.; Challacombe, M.; Gill, P. M. W.; Johnson, B.; Chen, W.; Wong, M. W.; Gonzalez, C.; Pople, J. A. *Gaussian 03* (Revision E.01); Gaussian, Inc.: Wallingford, CT, 2004.